energy&fuels

pubs.acs.org/EF

Article

Performance Assessment of Modeling Approaches for Moderate or Intense Low-Oxygen Dilution Combustion in a Scale-Bridging Burner

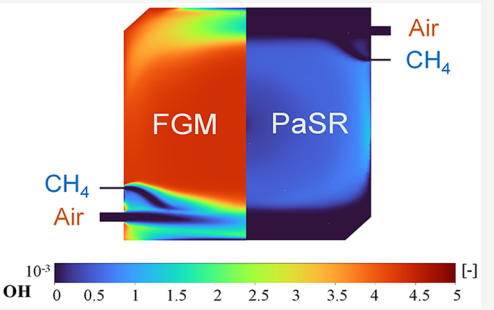
Lorenzo Giuntini, Lorenzo Frascino, Giovanni Battista Ariemma, Chiara Galletti, Giancarlo Sorrentino,* and Raffaele Ragucci

Cite This: *Energy Fuels* 2023, 37, 9500−9513

Read Online

ACCESS | Metrics & More | Article Recommendations | Supporting Information

ABSTRACT: The present work provides deep insights into methane oxidation in a cyclonic flow field chamber whose strong internal recirculation of burnt products enables the attainment of a moderate or intense low-oxygen dilution (MILD) combustion regime over a wide range of operating conditions. Steady-state Favre-averaged Navier−Stokes (FANS) simulations are performed to evaluate the thermochemical processes taking place within the reactor and to assess the suitability of existing computational fluid dynamics (CFD) models to describe the turbulence−chemistry interactions in such a scale-bridging configuration. A sensitivity analysis is carried out with respect to different turbulence closure models [i.e., renormalization group (RNG) $k-\varepsilon$, realizable $k-\varepsilon$, and Reynolds stress model], kinetic mechanisms (i.e., KEE-58 and GRI-Mech 2.11), as well as different turbulent combustion approaches, i.e., the flamelet generated manifold (FGM), the eddy dissipation concept (EDC), and the partially stirred reactor (PaSR) models. The accuracy of numerical predictions is assessed by a direct comparison to obtained experimental results in terms of temperature profiles locally collected within the reactor and flue gas compositions monitored at the exit of the burner. Results highlight that the EDC and PaSR methods are the most suitable modeling paradigms for the investigated MILD combustion conditions, although the former may likely predict an extinction of the combustion process; conversely, the FGM model shows the largest discrepancies with respect to experimental data, highlighting the need for improvements.



1. INTRODUCTION

Process efficiency, fuel and load flexibility, and net-zero pollutant emissions are key aspects to be considered in the design of new generation burners for heat and power generation in several sectors.

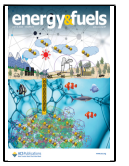
However, one of the key unsolved issues that would allow for a gradual transition into a carbon-neutral future using renewable energy vectors is the availability of conversion technologies that are able to ensure fuel-flexible operation, which is very challenging because of the vastly different combustion properties of alternative fuels with respect to fossil fuels (e.g., ammonia and natural gas). A particularly promising thermochemical conversion process in this perspective is moderate or intense low-oxygen dilution (MILD) combustion,[1] along with other related concepts, such as flameless combustion and colorless distributed combustion (CDC),[2] where high levels of preheating and dilution of the reactants by the exhaust gases lead to a combustion regime with small heat release that is characterized by high stability, increased fuel flexibility, and low emissions.

MILD combustion[1] is widely recognized as one of the most promising to efficiently convert a wide palette of energy carriers[3] while already having the appropriate technological readiness level to be considered a real solution to sustain the energy grid. In such a combustion regime, high dilution and preheating of fresh reactants entail the establishment of a distributed oxidation mainly controlled by local mixture ignition mechanisms under moderate temperatures instead of deflagrative/diffusive structures.[4] In fact, the high turbulence levels make the flame front thicken and stretch, so that chemical reactions are no longer confined in a thin layer but take place volumetrically under locally hot and diluted mixture conditions.[5]

These peculiar inherent features lead to a uniform temperature field without peaks, an invisible and noiseless reactive region, negligible soot formation, large fuel flexibility and very low NO_x, CO, and unburned emissions.[1,6−8]

Despite these advantages, the broad implementation of MILD combustors in different industrial sectors is still limited as a

Received: February 22, 2023
Revised: June 8, 2023
Published: June 26, 2023



ACS Publications

© 2023 The Authors. Published by American Chemical Society

https://doi.org/10.1021/acs.energyfuels.3c00597
Energy Fuels 2023, 37, 9500−9513

Downloaded from pubs.acs.org/enfuem/article-pdf/37/13/9500/1023331/ef3c00597.pdf by guest on 28 August 2026

result of the weak and limited knowledge of the physical and chemical phenomena occurring in such an oxidation regime.[9−11] In this scenario, the availability of numerical models, based on computational fluid dynamics (CFD), may strongly help improve this knowledge and promote the required technological advancement. However, CFD models have been developed and optimized for conventional combustion; therefore, significant effort is required to make them suitable for MILD conditions. Indeed, simple processes occurring in MILD conditions differ from those involved in conventional systems as a result of strong overlapping between stirring/mixing and chemistry effects. Flue gas entrainment induces high local diluent levels, so that chemical kinetics become slow enough to operate on time scales comparable to mixing time scales.[9] Therefore, the turbulence/chemistry interaction needs to be considered with appropriate and effective turbulent combustion models.[12,13] Classical turbulent combustion modeling paradigms related to the flamelet/non-flamelet concepts seem to be questionable when applied to distributed reaction zones for both the Reynolds-averaged Navier−Stokes (RANS) and large eddy simulation (LES) environments.[14] The decrease of kinetic rates leads to a low Damkhöler number that approaches unity.[15] Therefore, the introduction of detailed chemistry seems to be of paramount importance for the design and optimization of such systems. Consequently, accurate models for describing both the turbulent stirring/mixing and kinetics and their interactions must be included in the CFD modeling. Satisfactory predictions for turbulent combustion modeling of MILD systems are reported in the literature for flamelet-based models.[16] In comparison to the eddy dissipation concept (EDC) model or its modified versions,[17,18] which is widely used for modeling of MILD combustion,[19] tabulated chemistry models [such as the flamelet generated manifold (FGM)] are computationally very efficient.[20]

Some recent studies also showed quite good modeling performance when finite-rate combustion models based on a partially stirred reactor (PaSR) approach are employed.[21]

Despite the modeling efforts reported in the literature, the non-conventional reactive region structure advocates the need for novel approaches for MILD regime or proper modification/tuning of the existing approaches. The underlying physical mechanisms are not yet fully understood, and the validation of combustion models featuring enhanced predictive capabilities is required.

In this context, the development of comprehensive modeling tools requires active interconnections between experiments and computations for the model assessment. In this regard, several facilities, such as the jet-in-hot-coflow (JHC)[22,23] and the Cabra flame,[24] were used in the past to mimic highly diluted and preheated conditions. The adoption of advanced diagnostic tools to obtain information on the main variables (e.g., species compositions, temperature, and velocity) represented a strong asset for the validation of the models.[25] Nonetheless, in industrial applications, MILD combustion is achieved through massive burnt gas recirculation, which allows for dilution of the inlet mixture before its ignition. The specific design of the inlet jet aerodynamics together with a tailored flow field inside the combustion chamber permits the acquisition of the desired recirculation degree.[26] The local dilution strongly affects mixing and chemical scales, making such configurations deeply different from JHC and Cabra configurations, which are only based on the modification of the kinetics time scale. In fact, other representative characteristics of MILD combustion commonly found in burners with an internal exhaust gas recirculation (EGR) are absent in the JHC configuration. In this respect, lab-scale burners[27,28] and semi-industrial furnaces[29−32] reported in the literature highlight the key role of combustion product recirculation to ensure dilution and preheating of fresh reactants essential to attain MILD combustion conditions.

Therefore, the morphology of the turbulent MILD reaction zone needs to be investigated with proper scale-bridging configurations, showing quasi-industrial features while ensuring a very accurate control of both boundary and operating conditions.

In this framework, the present study aims at characterizing, both experimentally and numerically, the main features characterizing MILD combustion of methane in a scale-bridging system, i.e., a cyclonic flow reactor with internal EGR.[33] Such a configuration shares important similarities with the intended applications (boilers, gas turbines, and furnaces), without the complex interactions characterizing the industrial systems. This is crucial to provide the necessary scale-bridging information from the laboratory units to the real applications and to allow for the validation of physical submodels.

Temperature measurements and flue gas compositions were collected for three different inlet operative conditions and were used as experimental data for model validation. The combustion process was numerically modeled by CFD techniques based on RANS simulations, bringing attention to the choice of the turbulent combustion model. Three different modeling paradigms were investigated: a tabulated chemistry approach, i.e., the FGM,[34] and two reactor-based models, i.e., the EDC, in its standard[35] and modified formulations,[13,17−19] and the PaSR model,[36] with various mixing constant values.

Obtained results from such an experimental/numerical cross-validation procedure will allow for assessment of the performance of MILD modeling paradigms with respect to their reliability for the design of innovative burner concepts based on MILD technology in different fields.

2. EXPERIMENTAL APPARATUS

The reactor employed for the experimental investigation is the laboratory unit cyclonic burner (LUCY) developed at STEMS−CNR, extensively described in previous works.[28,37,38] Briefly, as illustrated in Figure 1, the burner consists of an atmospheric 2000 cm^3 prismatic combustion chamber, equipped with an antisymmetrical reactant feeding system consisting of two couples of oxidizer and fuel nozzles, placed orthogonally with respect to the outlet section, which is located in the center of the bottom face of the reactor. Such a peculiar

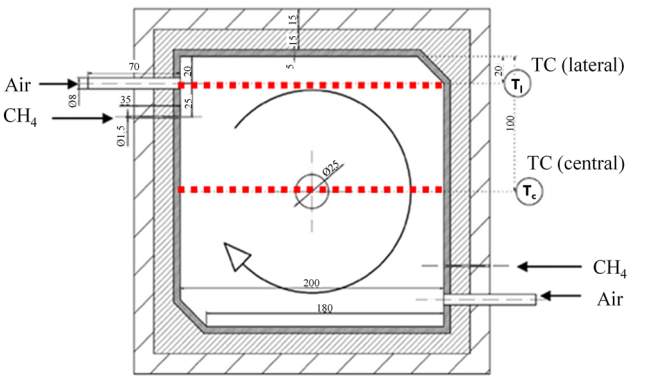


Figure 1. Sketch of the LUCY reactor with thermocouple locations along the red lines.

Downloaded from pubs.acs.org/enfuem/article-pdf/37/13/9500/1023331/ef3c00597.pdf by guest on 28 August 2026

https://doi.org/10.1021/acs.energyfuels.3c00597
Energy Fuels 2023, 37, 9500−9513

design allows for the establishment of a cyclonic flow field, which ensures a strong internal recirculation of mass and sensible enthalpy, by diluting the fresh reactants and increasing the temperature above the autoignition temperature. The resulting formation of hot gas/fresh reactant mixtures with local conditions of high dilution and preheating allow for the establishment of MILD combustion conditions for each case study investigated in this work.

The experimental campaign aimed at analyzing the combustion characteristics of methane/air mixtures, at different equivalence ratios (ϕ), i.e., ϕ = 1.0, 0.8, and 0.6. Specifically, pure methane was fed to the combustion chamber with a mass flow rate corresponding to a thermal power input of 7 kW for all of the investigated conditions, whereas the oxidizer was fed regulating its flow rate depending upon the desired equivalence ratio. The experimental setup allows for the collection of temperature and exhaust gas composition data. In particular, two movable N-type thermocouples are placed on the midplane of the burner, to detect axial temperature profiles in the reactant mixing region (T_l) and in the recirculation region (T_c), respectively. A third N-type thermocouple is placed at the exit to measure the characteristic exhaust temperature.

Besides, the cyclonic burner is placed within a refractory wall confinement, in which a constant flow rate of inert species (N_2 in the current study) is fed, to prevent the formation of explosive stagnation zones. Such a configuration entails a continuous convective heat exchange between the burner walls and the inert stream, whose temperature of 500 K was continuously measured during the experimental campaign. Therefore, in the following numerical simulations, a convective heat transfer boundary condition with a fixed external bulk temperature was considered to be the most appropriate for the present case study. In particular, the fixed convective heat transfer coefficient used for simulations was also verified on the basis of the measured exit flow temperatures.

In addition, a water-cooled probe, followed by a water condensation trap, was mounted at the exit of the burner to monitor the exhaust gas composition.

An Agilent micro gas chromatograph (GC) gas analyzer was employed to determine the molar fractions of the main species (CH_4, O_2, CO_2, H_2, and CO). Additional information about the experimental setup and instrumentation can be found in refs 28 and 37.

3. NUMERICAL MODEL

Favre-averaged Navier−Stokes (FANS) equations for the conservation of mass, momentum, and energy in their steady-state formulation were solved by employing the commercial code Ansys Fluent 19.3, based on finite volume methods

$$\nabla(\overline{\rho}\tilde{\mathbf{u}}) = 0 \tag{1}$$

$$\nabla(\overline{\rho}\tilde{\mathbf{u}}\tilde{\mathbf{u}}) = -\nabla\overline{p} + \nabla\overline{\mathbf{T}} - \nabla(\overline{\rho}\widetilde{\mathbf{u}''\mathbf{u}''}) \tag{2}$$

$$\nabla(\overline{\rho}h\tilde{\mathbf{u}}) = \nabla(\overline{\rho}\alpha\nabla h) - \nabla(\overline{\rho}\widetilde{h''\mathbf{u}''}) - \overline{\sum_{1}^{N} h_k\dot{\omega}_k} + \overline{Q_{rad}} \tag{3}$$

where $\tilde{\phi}$ and ϕ'' are the Favre average and the fluctuation of a generic variable ϕ, respectively. In the above set of equations, $\mathbf{u}$, p, $\mathbf{T}$, and h are the velocity vector, the pressure, the stress tensor, and the enthalpy, respectively, while ρ represents the density and α represents the thermal conductivity.

The internal gas recirculation induced by the cyclonic motion inside the reactor produces high turbulence levels, flow separations, and strong mixing phenomena between fresh reactants and hot/diluted products. For these reasons, turbulence modeling in such a combustion system is a key aspect requiring great attention; hence, different turbulence models were considered in the analysis to close the Reynolds stress tensor, i.e., $\overline{\rho}\widetilde{\mathbf{u}''\mathbf{u}''}$. More precisely, the renormalization group (RNG) $k-\varepsilon$ model,[39] with the swirl-dominated flow option activated, and the Reynolds stress model (RSM) are applied. In near wall regions, special attention was paid to ensure an adequate mesh quality, because separation and reattachment of the flow was expected. Moreover, it is worth noting that the reactor does not present a large bulk volume; therefore, most zones are strictly influenced by walls. For this reason, in the mesh generation process prism layers were created at the walls and a $y^+ < 1$ was ensured in all simulations. This allowed for the boundary layer to be solved with the enhanced wall treatment, hence avoiding the use of wall functions. The impact of chemistry on the results was analyzed using different kinetic schemes: the GRI-Mech 2.11 (31 species and 175 reactions),[40] without the nitrogen chemistry, the KEE-58 (17 species and 58 reactions),[41] the AramcoMech 3.0 (581 species and 3037 reactions),[42] and the San Diego mechanism (58 species and 271 reaction).[43] The radiative transport equation (RTE) was modeled with the discrete ordinates (DO) model,[44] discretizing each octant of the angular space with 5 × 5 solid angles and with a pixelation of 3 × 3, as recommended for periodic meshes by the Fluent Guide;[45] the spectral properties of the gas were evaluated with the weighted sum of gray gases (WSGG) model.[46]

Because the reactor operates in MILD combustion conditions with Damkhöler numbers, Da, close to unity, the conventional turbulence−chemistry interaction (TCI) models used in the literature for flame conditions might provide incorrect predictions, being that such combustion models originally developed for traditional flames having $Da \gg 1$. Hence, we tested different TCI models, both in their standard[35,36] and modified formulations for MILD/flameless combustion systems;[12,13,17−19] these modeling approaches are presented in the following subsections.

3.1. TCI Modeling. *3.1.1. Flamelet Generated Manifold (FGM) Model.* FGM is a TCI model based on a flamelet approach; i.e., the turbulent flame structure is approximated with an ensemble of laminar and locally one-dimensional flames driven by the turbulent flow field in which they are immersed.[47,48] It allows for the description of combustion regimes exhibiting features of both premixed, partially premixed, and non-premixed modes.[47,48] On the basis of the flamelet hypothesis, scalar quantities, such as the temperature and species mass fractions, can be determined on the basis of a few controlling variables, thus allowing for an important reduction of the degrees of freedom of the initial thermochemical state of the system.[49]

In this case, three controlling variables were selected: the mixture fraction (Z) to describe mixing between the fuel and oxidizer, the progress variable (C) representing the progress of the reaction, and the enthalpy for non-adiabatic calculations. One-dimensional equations for flamelets are preprocessed, and the thermochemical quantities are stored in tables as functions of the three controlling variables. In the subsequent CFD simulations, only the controlling variables are transported, thus reducing by orders of magnitude the computational efforts; in fact, with this approach, the mass fractions are retrieved from tables in a look-up procedure, avoiding the resolution of a transport equation for each species.

3.1.2. Eddy Dissipation Concept (EDC) Model. The EDC is a finite-rate chemistry model originally developed by Magnussen.[35] This model assumes that the reaction occurs in fine structures, i.e., small turbulent scales having dimensions comparable to the Kolmogorov length, which are immersed in non-reacting zones, called surroundings. These reacting

Downloaded from pubs.acs.org/enfuem/article-pdf/37/13/9500/1023331/ef3c00597.pdf by guest on 28 August 2026

https://doi.org/10.1021/acs.energyfuels.3c00597
Energy Fuels 2023, 37, 9500−9513

structures are considered as locally homogeneous and approximated to a perfectly stirred reactor; the fraction of the fluid occupied by such structures (γ^*) and the fine structure residence time (τ^*) are expressed as

$$\gamma^* = C_\gamma \left(\frac{\nu\varepsilon}{\kappa^2}\right)^{1/4} \quad (4)$$

$$\tau^* = C_\tau \left(\frac{\varepsilon}{\nu}\right)^{1/2} \quad (5)$$

where ν, κ, and ε are the kinematic viscosity of the fluid, the turbulent kinetic energy, and its dissipation rate, respectively, while C_γ and C_τ are model constants equal to 2.1377 and 0.4082, respectively.

The EDC model can incorporate a detailed kinetic mechanism by solving a transport equation for each chemical species, thus resulting in high computational costs. In the past, EDC was employed successfully to predict turbulent reacting flows characterized by $Da > 1$.

However, when EDC was applied to systems operating under MILD combustion conditions, i.e., with Damköhler approaching unity, it demonstrated unsatisfactory results, and model revisions were proposed. The modifications were mainly focused on the tuning of the model constants C_γ and C_τ to fit detailed experimental data on JHC concepts emulating MILD combustion. Aminian et al.[50] proposed to increase C_τ from its standard value up to 1.5; Evans et al.[13] adjusted both model constants, setting C_τ to 1 and C_γ to 3. Recently, Parente et al.[17] presented a more sophisticated method to adapt the model constants depending upon the Damkhöler number at the Kolmogorov scale (Da_η) and the turbulent Reynolds number (Re_t), resulting in a more general approach.

In this work, both the EDC standard and the EDC with modified constants according to Aminian et al.[18] are employed. It is worth nothing that modeling studies on the LUCY burner demonstrated that the Evans[13] modification leads to global extinction of the flame, because of the very high value of C_τ; hence, such results are not reported.

3.1.3. Partially Stirred Reactor (PaSR) Model. The PaSR model developed by Chomiak et al.[36] does not consider the fine structures like in the EDC model but assumes that each computational cell is divided into reactive and non-reactive parts, where the fraction of the former explicitly depends upon mixing and chemical time scales estimated globally, i.e., τ_m and τ_c, respectively. More precisely, τ_c is obtained from the ratio between the mass fraction and the formation rate of representative species, while τ_m can be estimated with a static or dynamic approach. Although the dynamic method is conceptually more accurate, previous studies demonstrated very small differences in the predictions of the two methods.[10,51] For this reason, in this work, the static method was applied, also to save computational time, which expresses the mixing time as $\tau_{mix} = C_{mix}k/\varepsilon$, where C_{mix} is a mixing constant typically set to the value of 0.5, but more in general, it can vary in the range of 0.1−1. Indeed, higher or lower C_{mix} values are representative of less or more intense mixing conditions, respectively; these directly influence the mixing time scale and, thus, the mean reaction rate.

In summary, the main difference between EDC and PaSR lies in the estimation of the fraction of the reactive structures. In EDC, such a fraction is solely based on turbulence quantities, while in PaSR, the reacting fraction explicitly depends upon both the mixing and chemical time scales. For this reason, the PaSR model typically works better than the standard EDC model especially for combustion conditions, in which detailed chemistry plays a key role, like in the MILD regime.

3.2. Numerical Setup. The computational domain considers half of the LUCY burner, as shown in Figure 2. This

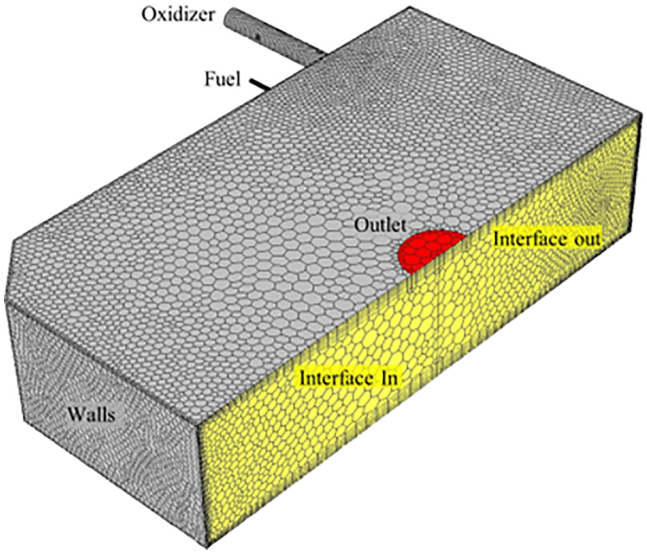


Figure 2. Computational grid with periodic boundary conditions.

was made possible by exploiting the antisymmetry of the geometry, introducing a rotational periodicity, which allowed for strong reduction of the numerical efforts. A grid sensitivity analysis was carried out comparing four grids to the number of cells ranging from 135 000 to 440 000. The selected mesh consists of about 300 000 elements, with polyhedrons in the bulk and five prism layers at the walls. Local refinements are applied at the nozzle exits and close to the walls, with these being the most important regions for mixing, chemical reactions, and heat exchange.

With regard to the boundary conditions, uniform values of inlet velocity magnitude, temperature (T_{in}), and composition at the fuel and air inlets were set, as reported in Table 1. A periodic

Table 1. Boundary Conditions

stream	ϕ	v (m/s)	T_{in} (K)	CH_4 (vol %)	N_2 (vol %)	O_2 (vol %)
fuel		61.79	300	100	0	0
oxidizer	1.0	39.98	583	0	79	21
	0.8	46.97	548	0	79	21
	0.6	52.11	456	0	79	21

boundary condition with a rotation of 180° was applied at the two interfaces shown in Figure 2. To mimic the heat exchanged through the surroundings, a convective heat transfer condition was imposed at the reactor walls. In particular, an external free stream bulk temperature of 500 K was applied, while the heat transfer coefficient, h, was adjusted in the range of 30−70 W m^{-2} K^{-1} to meet the experimental measured flue gas temperatures at the burner exit. We noticed how the highest values of h were required for $\phi = 1.0$ and the lowest values of h were required for $\phi = 0.6$. As a result of the low Mach numbers within the reactor, the low operating pressure, and high temperatures, the gas was assumed to be incompressible and ideal. For the solution procedure, a double precision, pressure-based solver was chosen.

https://doi.org/10.1021/acs.energyfuels.3c00597
Energy Fuels 2023, 37, 9500−9513

Downloaded from pubs.acs.org/enfuem/article-pdf/37/13/9500/1023331/ef3c00597.pdf by guest on 28 August 2026

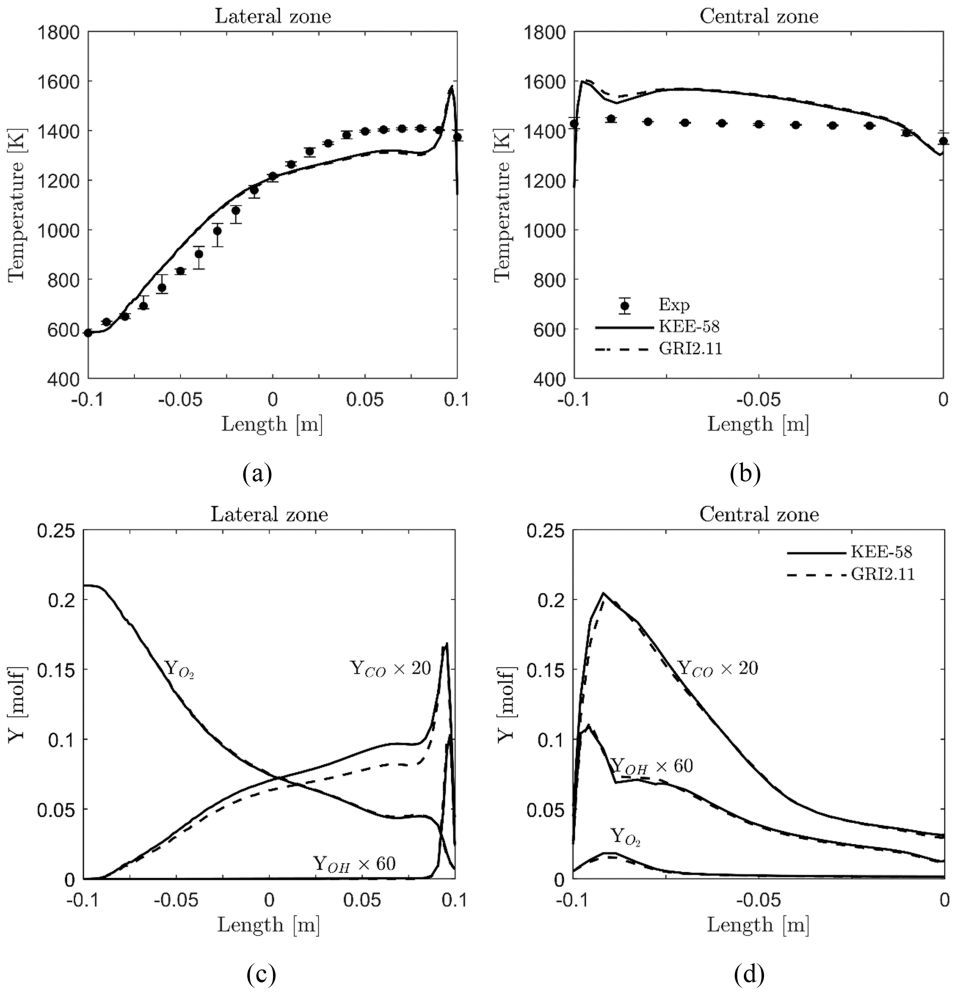


Figure 3. Profiles of the temperature (plots a and b) and molar fraction of O_2, CO, and OH (plots c and d) along the lateral (left) and central (right) zones for the base case, i.e., $\phi = 1$. Comparison of kinetic schemes, KEE-58 and GRI-Mech 2.11, employing RNG $k-\varepsilon$ as a turbulence model and the standard EDC as a combustion model.

Table 2. Temperature and Dry Species Molar Fractions in the Exhaust Gas Predicted with Different Kinetic Schemes for the Base Case, i.e., $\phi = 1.0$

case	data	T_{out} (K)	CH_4 (ppm)	H_2 (ppm)	CO (ppm)	CO_2 (%)	O_2 (%)
$\phi = 1.0$	EDC_{std}, GRI-Mech 2.11	1371	0	1521	1839	11.51	0.17
	EDC_{std}, KEE-58	1368	1	1439	1858	11.50	0.19

The FANS equations were solved with the SIMPLE algorithm for the pressure−velocity coupling and the PRESTO! option for pressure discretization. All other transport equations were discretized with second-order upwind schemes. Gradients were calculated with the least squares method. The convergence of the solution was identified by monitoring the temperature and species at the outlet and ensuring stable residuals below 10^{-6}.

4. RESULTS AND DISCUSSION

Numerical simulations based on CFD techniques (and implementing different submodels) were performed to evaluate their reliability with respect to methane MILD combustion. Specifically, a sensitivity analysis was carried out with respect to different kinetic mechanisms and turbulence models, by choosing the case at $\phi = 1$ as the benchmark and comparing them to experimental evidence. Specifically, GRI-Mech 2.11[40] and KEE-58[41] were chosen as reference kinetic mechanisms, while the EDC standard and with modified $C_\tau = 1.5$, PaSR with $C_{mix} = 0.5$, and FGM were investigated as different combustion paradigms. Furthermore, the best combinations of models identified in such preliminary analyses were validated against experimental data at $\phi = 0.8$ and 0.6.

In the following, results are discussed in terms of the lateral and central zones of the combustion chamber, referring to those obtained with respect to T_l and T_c, respectively.

4.1. Sensitivity Analysis: Kinetic Mechanism. Figure 3 displays experimental and numerical profiles of the temperature (plots a and b) together with numerical profiles of O_2, CO, and OH molar fractions (plots c and d), along the lateral and central regions, as a function of the axial position within the combustion chamber. In particular, the axial coordinate of −0.1 m corresponds to the reactor wall where the reactants inlets are placed, whereas 0.1 m is the opposed wall, respectively. For the predictions, different kinetic schemes, i.e., GRI-Mech 2.11 and KEE-58, with standard EDC and the RNG $k-\varepsilon$ model are employed. The results show practically overlapping profiles for

https://doi.org/10.1021/acs.energyfuels.3c00597
Energy Fuels 2023, 37, 9500−9513

Downloaded from pubs.acs.org/enfuem/article-pdf/37/13/9500/1023331/ef3c00597.pdf by guest on 28 August 2026

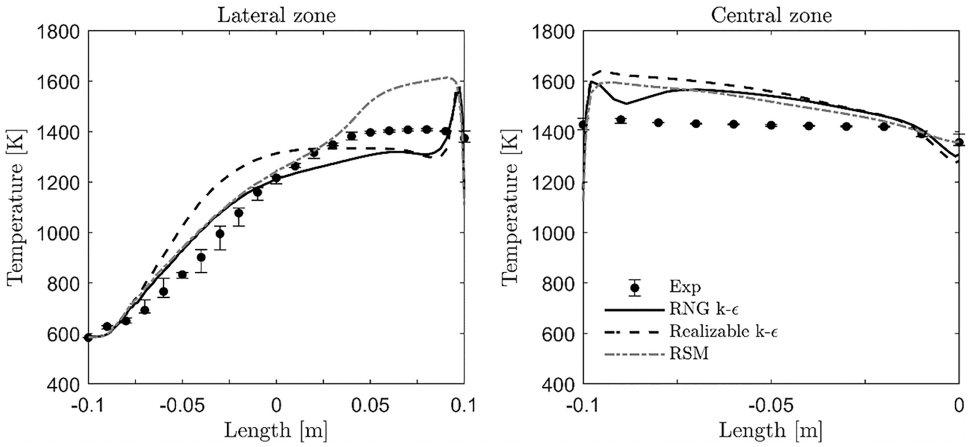


Figure 4. Temperature profiles along the lateral (left) and central (right) thermocouples for the base case, i.e., $\phi = 1$. Comparison of turbulence models: RNG $k-\varepsilon$ model, realizable $k-\varepsilon$ model, and RSM, with KEE-58 as a kinetic scheme and EDC standard as a combustion model.

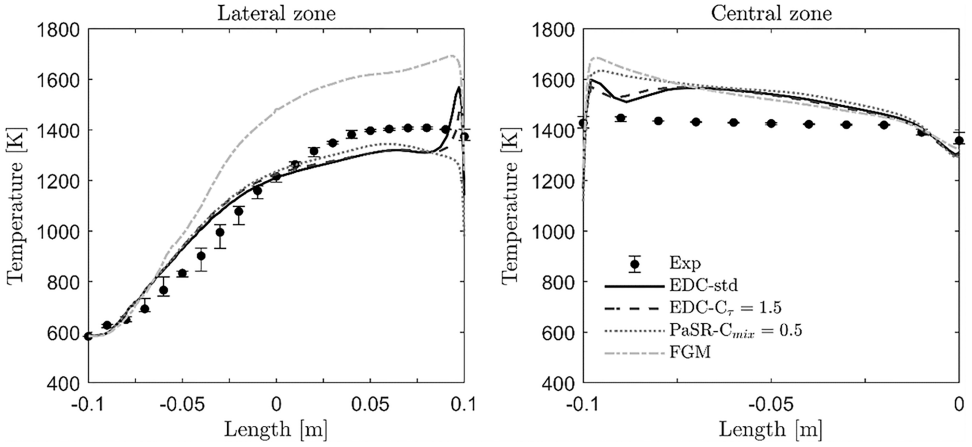


Figure 5. Temperature profiles along the lateral (left) and central (right) thermocouples for the base test case, i.e., $\phi = 1$. Comparison of TCI models: EDC standard, EDC with $C_\tau = 1.5$, PaSR with $C_{mix} = 0.5$, and FGM, with KEE-58 as a kinetic scheme and RNG $k-\varepsilon$ as a turbulence model.

both the temperature and species, with a general good agreement with the experimental data of the temperature. To provide an even more comprehensive evaluation, exhaust gas compositions predicted by the two mechanisms are reported in Table 2, showing practically negligible differences in the values predicted. In addition, more detailed kinetic mechanisms were also tested (AramcoMech 3.0[42] and San Diego mechanism[43]) using FGM, which allows for the inclusion of detailed chemistries with affordable computational costs. In this respect, obtained results, reported in section 1 of the Supporting Information for the sake of brevity, show no evident improvements with respect to the KEE-58 and GRI-Mech 2.11 mechanisms.

Therefore, KEE-58 was selected for the following analyses because it requires a much lower computational effort with respect to the more detailed GRI-Mech 2.11 scheme.

4.2. Sensitivity Analysis: Turbulence Models. Figure 4 presents the temperature profiles along the lateral and central thermocouples obtained with the realizable $k-\varepsilon$ model, the RNG $k-\varepsilon$ model, and the RSM in combination with KEE-58 and the standard EDC. Hence, we remark the importance of the sensitivity analysis to the turbulence model, especially when the thermal field is highly influenced by the velocity field, as in this case study. Looking at the results of Figure 4, it can be noticed that the RNG $k-\varepsilon$ model and the RSM perform likewise in the first half of the lateral zone, for a length in the range of $-0.1 < x <$ 0 m. In this region, such models slightly overestimate the experimental data by about 50 K on average. On the contrary, the realizable $k-\varepsilon$ model overpredicts the air preheating in this region. In the second half of the reactor length, the realizable $k-\varepsilon$ model shows similarities to the RNG $k-\varepsilon$ model, and both models slightly underpredict the experimental data, whereas the RSM overpredicts the experimental data. In this region, the interaction between the turbulence model and the combustion model becomes crucial. Concerning the central zone, all turbulence models can predict the uniformity of the temperature field within the burner, despite an average offset of about 100 K from the experimental points.

In general, the RNG $k-\varepsilon$ model and RSM provide comparable and satisfactory performance in most regions of the burner, while the realizable $k-\varepsilon$ model shows worse agreement with the experimental data; hence, for the sake of brevity, only the results with the RNG $k-\varepsilon$ model will be presented in the following paragraphs. Moreover, the RNG $k-\varepsilon$ model is more optimized than the RSM for this case study, because the latter presents more equations to solve, resulting in higher computational costs and numerical convergence issues.

4.3. Sensitivity Analysis: Turbulence–Chemistry Interaction (TCI) Models. The standard EDC with the chosen turbulence model and kinetic scheme can satisfy the overall trends of the temperature, but some discrepancies with the experimental data are still present. For this reason, other TCI

Downloaded from pubs.acs.org/enfuem/article-pdf/37/13/9500/1023331/ef3c00597.pdf by guest on 28 August 2026

https://doi.org/10.1021/acs.energyfuels.3c00597
Energy Fuels 2023, 37, 9500−9513

Table 3. Temperature and Dry Species Molar Fractions in the Exhaust Gas, Predicted by the Numerical Models and Measured in the Experiments for the Case ϕ = 1.0

case	data	T_{out} (K)	CH_4 (ppm)	H_2 (ppm)	CO (ppm)	CO_2 (%)	O_2 (%)
ϕ = 1.0	EXP	1358	403	2910	4160	11.20	0.34
	EDC_{std}	1368	1	1439	1858	11.50	0.19
	EDC_{mod}	1361	2	1450	1890	11.49	0.20
	PaSR C_{mix} = 0.5	1362	178	1360	2009	11.44	0.26
	FGM	1368	1	4974	11930	10.06	1.18

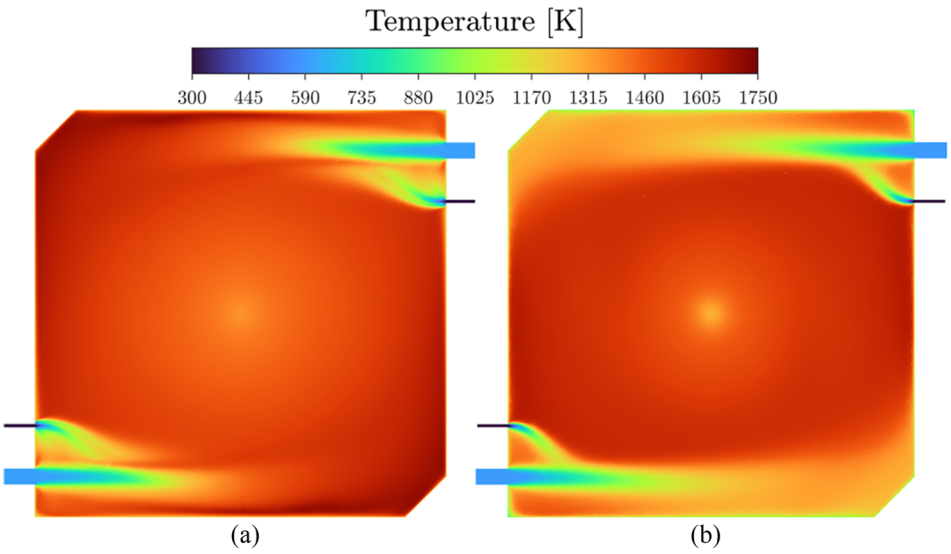


Figure 6. Contours of the temperature (K) for FGM (a) and PaSR with C_{mix} = 0.5 (b) for the base case, i.e., ϕ = 1, with KEE-58 as a kinetic scheme and RNG $k-\varepsilon$ as a turbulence model.

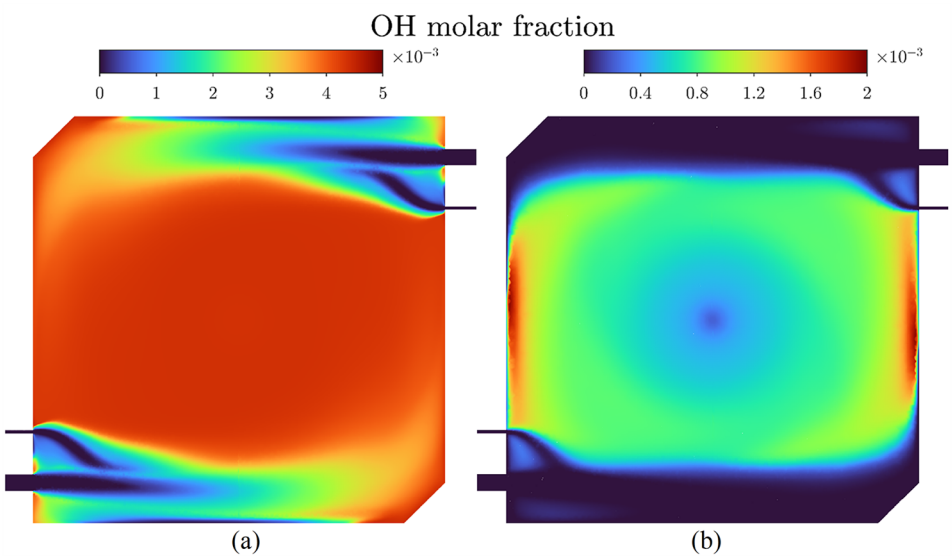


Figure 7. Contours of the molar fraction of OH for FGM (a) and PaSR with C_{mix} = 0.5 (b) for the base case, i.e., ϕ = 1, with KEE-58 as a kinetic scheme and RNG $k-\varepsilon$ as a turbulence model.

models can lead to a further improvement of the accuracy and, hence, need to be tested. In Figure 5, the comparison between the standard EDC, the EDC with the modification proposed by Aminian et al.,[50] the PaSR model with mixing constant C_{mix} = 0.5, and the FGM is shown. In addition, the Evans modification of EDC[13] was also tested, but it was not possible to achieve stable flame conditions because a global extinction occurred for each test case reported here.

The temperature profiles predicted by EDC with modified C_τ are quite similar to those predicted by standard EDC (profiles almost overlap), in both the lateral and central zones, and hence, the same considerations apply. Even the PaSR model with C_{mix} = 0.5 presents similar trends, although it shows a slightly better agreement with the experimental data in the second half of the lateral zone length, and moreover, it does not present any peak of the temperature close to the wall of the reactor, i.e., at about 0.1

https://doi.org/10.1021/acs.energyfuels.3c00597
Energy Fuels 2023, 37, 9500−9513

Downloaded from pubs.acs.org/enfuem/article-pdf/37/13/9500/1023311/ef3c00597.pdf by guest on 28 August 2026

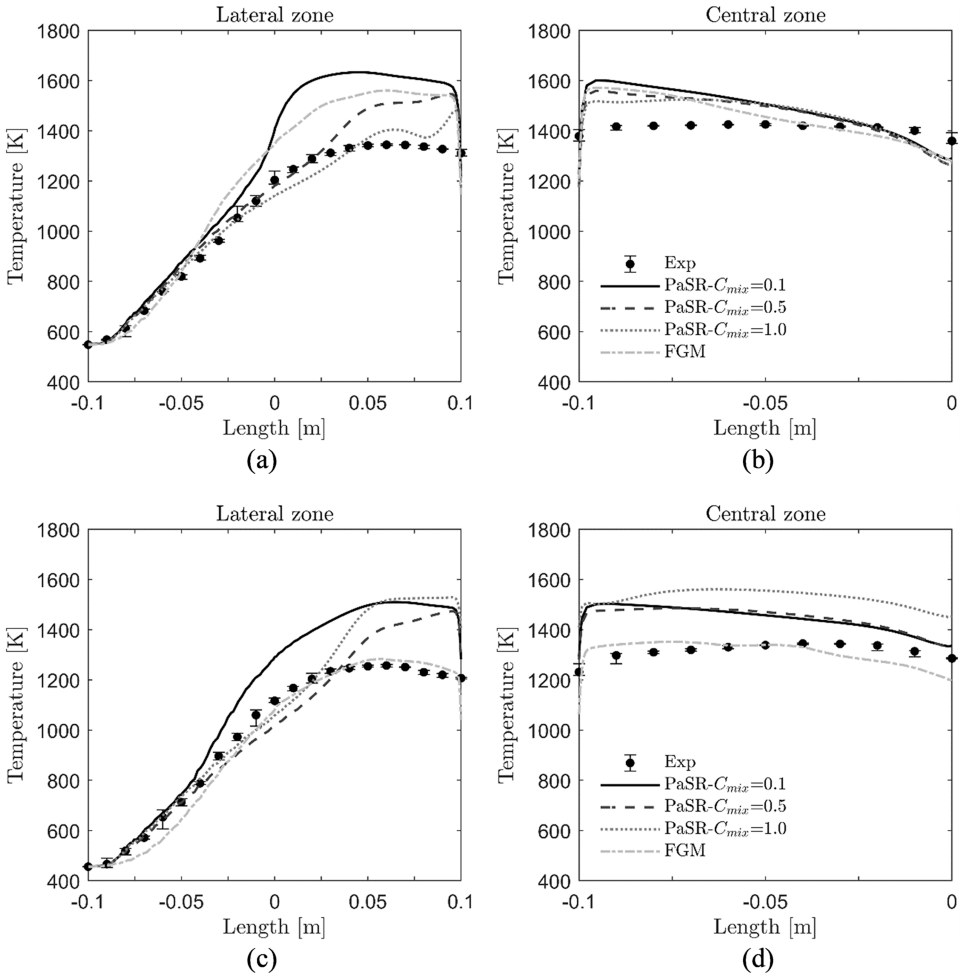


Figure 8. Temperature profiles along the lateral (left) and central (right) thermocouples for the cases with ϕ = 0.8 (plots a and b) and ϕ = 0.6 (plots c and d). Comparison of TCI models: FGM and PaSR with C_{mix} = 0.1, 0.5, and 1.0, with KEE-58 as a kinetic scheme and RNG $k-\varepsilon$ as a turbulence model.

m. On the other hand, FGM largely overestimates the temperature along the lateral zone, especially for $x > 0$ m, with a maximum overprediction of about 200 K. Recent studies showed that such temperature overpredictions can be related to the lack of an additional controlling variable in the lookup table creation to appropriately consider the ignition process of locally preheated and diluted mixtures.[52,53,52,53] Such an effect is emphasized in the present cyclonic flow reactor as a result of the high levels of burnt gases interacting with the fresh inlet mixture by modifying its thermochemical manifold state.[54] However, this effect influences the FGM prediction capabilities only along the peripheral region of the reactor, where ignition happens. Concerning the central zone, all models can predict a quite uniform temperature field, although not as much as that shown by the experimental measurements, which is completely flat.

The comparison among several used TCI models with respect to the local temperature profile predictions were also performed by evaluating the numerical−experimental discrepancies following the methodology proposed by Hu et al.,[55] reported in section 2 of the Supporting Information, and confirming the evidence reported in Figure 5.

Table 3 reports temperatures (T_{out}) and emissions of CH_4, H_2, and CO measured in the experiments and calculated in the CFD simulations at the outlet of the reactor. The molar fractions are presented on a dry basis. Looking at the results reported in Table 3, we notice how the numerical values show some discrepancies when compared to the experimental values. Specifically, both the EDC and PaSR models underestimate all of the species at the exit; however, the PaSR approach predicts CH_4, H_2, and CO emissions with values that are about half of the measured values, thus resulting in a relatively good agreement. On the other hand, FGM strongly overestimates CO and H_2, whereas it underestimates CH_4 concentrations.

Despite such differences in the species concentrations, T_{out} predicted values are very close for all of the models to the measured value, thus implying a different location and amplitude of the reactive region inside the reactor for the different modeling paradigms.

Figures 6 and 7 show the contours of the temperature and mole fraction of OH on the midplane of the burner. The temperature field is rather uniform within the reactor, especially that predicted by PaSR; in fact, FGM shows higher values of the temperature, especially close to the walls. Figure 8 shows that the OH field is also rather uniform, indicating that combustion is not localized but occurs volumetrically. Despite the uniformity captured by both models, FGM shows values of OH intensity much higher than those provided by PaSR, pointing out that the former predicts more intense combustion conditions.

Moreover, in Figure 7, it is well-visible that each model predicts the flame ignition occurring at different axial locations,

Downloaded from pubs.acs.org/enfuem/article-pdf/37/13/9500/1023331/ef3c00597.pdf by guest on 28 August 2026

https://doi.org/10.1021/acs.energyfuels.3c00597
Energy Fuels 2023, 37, 9500−9513

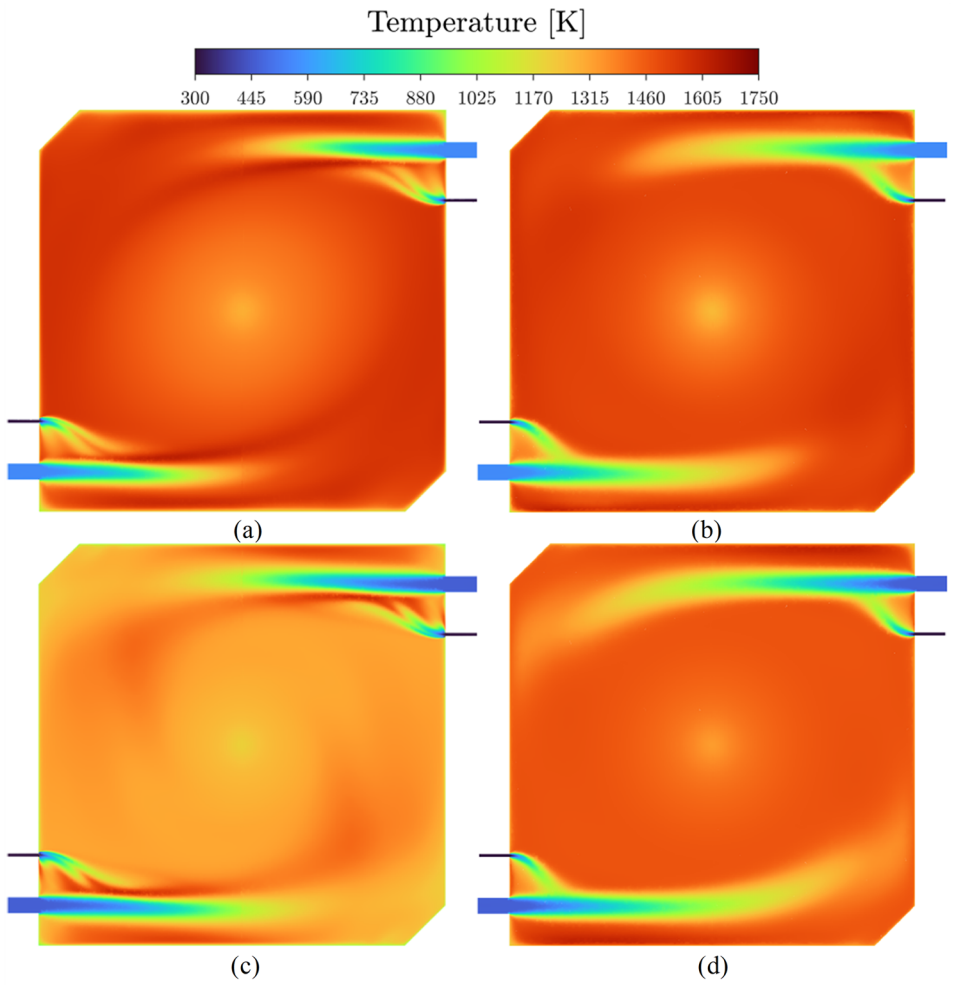


Figure 9. Contours of the temperature (K) for FGM (left) and PaSR with C_{mix} = 0.5 (right) for the cases with ϕ = 0.8 (contours a and b) and ϕ = 0.6 (contours c and d), with KEE-58 as a kinetic scheme and RNG $k-\varepsilon$ as a turbulence model.

showing that OH radicals are massively produced along the lateral axis according to FGM, while there is no flame in such a region according to PaSR. This explains why the lateral profiles of the temperature reported in Figure 5 present very specific shapes especially close to the wall of the burner, i.e., at about 0.1 m. For instance, FGM predicts an early ignition resulting in high temperatures in the range of $0 < x < 0.1$ m. On the other hand, EDC and PaSR show a more delayed ignition, which occurs just before the wall, i.e., at $x = 0.1$ m, for the former, whereas it occurs even further downstream for the latter with the peak of the temperature not being captured by the lateral axis.

In summary, the EDC and PaSR models show comparable performances, with the latter providing slightly better results in terms of temperature profiles and emission estimation. In addition, we must say that the standard EDC model and especially the EDC model with modified constants are more prone to predicting global flame extinction compared to PaSR, which, in turn, could benefit from C_{mix} tuning. Consequently, EDC models will not be discussed further in the subsequent sections as a result of their tendency toward global flame extinction at lower equivalence ratios and temperatures for the present case study.

On the other hand, FGM presents a different mathematical formulation with respect to the other models, i.e., EDC and PaSR, providing different results that are worth presenting and discussing. Moreover, FGM is less likely to predict global extinction as a result of its tendency to overpredict the in-flame temperature under diluted combustion conditions. Hence, only PaSR and FGM are included in the following sections.

4.4. Model Validation: ϕ = 0.8 and 0.6. It is common practice to evaluate the performance of a model under different operating conditions to ensure its robustness and reliability. For this reason, the models presented in the previous paragraphs are now tested for different operating conditions, i.e., equivalence ratios of 0.8 and 0.6. Figure 8 shows, similar to the case at ϕ = 1.0, the comparison between the temperatures obtained from the simulations and those recorded in the experiments. Looking at plots a and b of Figure 8, we observe that all models show fairly good agreement with the experimental data along the first half of the lateral axis, where combustion is weak. However, only the PaSR model with C_{mix} = 0.5 and 1 can provide a good estimation of the temperature profile along almost all lateral length. In fact, the case with C_{mix} = 0.1 is representative of an excessively strong mixing, which produces an early ignition of the fuel, similar to what happens according to FGM. It is worth noting that along the central axis all models show similar performances, with the numerical profiles that are almost superimposed but present an offset with respect to the experimental data; nevertheless, they can all predict a certain uniformity in the temperature field, as also demonstrated for the case with ϕ = 1, shown in Figure 5.

https://doi.org/10.1021/acs.energyfuels.3c00597
Energy Fuels 2023, 37, 9500−9513

Downloaded from pubs.acs.org/enfuem/article-pdf/37/13/9500/1023331/ef3c00597.pdf by guest on 28 August 2026

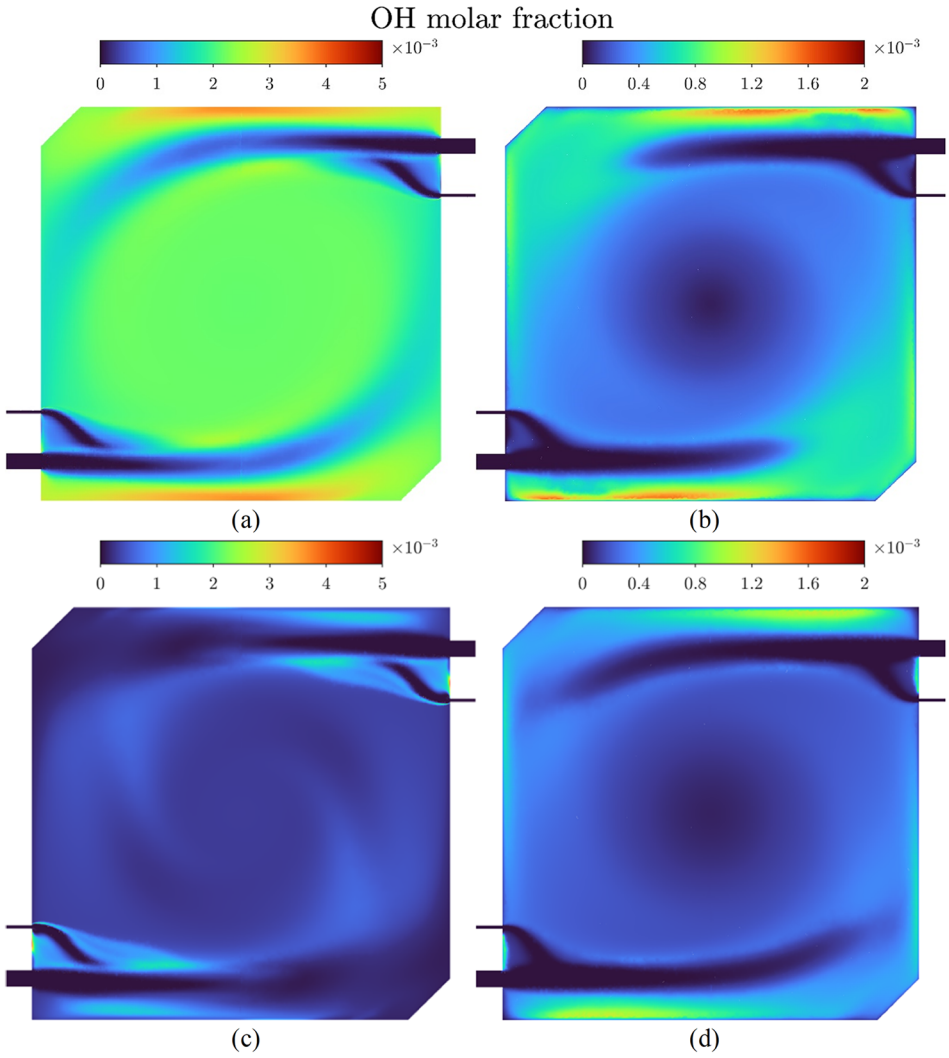


Figure 10. Contours of the molar fraction of OH for FGM (left) and PaSR with C_{mix} = 0.5 (right) for the cases with ϕ = 0.8 (contours a and b) and ϕ = 0.6 (contours c and d), with KEE-58 as a kinetic scheme and RNG $k-\varepsilon$ as a turbulence model.

Looking at the results for the case at ϕ = 0.6, reported in plots c and d of Figure 8, it can be observed that the FGM model achieves very good agreement with the experimental data, both along the lateral and central axes, in contrast with the other models tested. PaSR models globally overestimate the temperature within the reactor, especially in the central zone, showing a flat offset. Conversely, FGM can provide better predictions when compared to experimental data.

Figures 9 and 10 show the temperature and OH mole fraction fields for the cases at ϕ = 0.8 (a and b) and ϕ = 0.6 (c and d), predicted by FGM (left) and PaSR with C_{mix} = 0.5 (right), respectively. Looking at the results, it is evident how the maximum and average values of the temperature and OH become lower with the decrease of the equivalence ratio, as expected. Indeed, the more air fed to the reactor, the lower the temperature and OH concentration.

Observing the contours for both equivalence ratios, we see that the FGM predicts a zone of intense reaction, showing peaks of the temperature at the shear layer between the oxidizer and fuel jets, which are not visible according to PaSR. Indeed, for the former, most of the OH radicals are produced in such a mixing region, and then, they are distributed all over the reactor by the cyclonic motion. On the other hand, the PaSR model shows more evenly distributed scalar fields with smooth gradients, typical of MILD combustion conditions.

In addition, it must be noticed that FGM predictions improve at low equivalence ratios because, with more oxygen available within the reactor, the lack of a controlling variable considering the dilution effects as a result of recirculating products becomes less important. More precisely, in the case of confined cyclonic flows, such as the present MILD burner, the major source of disagreement for FGM can be ascribed to three-stream reactivity features, related to the interaction between the recirculating burnt products and the fresh gases. In particular, a relevant challenge in such approaches is to include in the manifold the effects of the recirculating burnt gases on the reactivity of the fresh mixture to properly represent the internal dilution effects. This is a very demanding task, which leads to expensive CFD simulations as a result of the high dimensionality of the look-up tables (up to 6D).

Hence, the increasing accuracy by decreasing ϕ for the FGM model is a result of the reduced effect of the internal dilution. Specifically, when the O_2 concentration at the inlet is high, such as for the case at ϕ = 0.6, FGM shows a good accuracy with respect to the experimental data, because internal dilution effects

Downloaded from pubs.acs.org/enfuem/article-pdf/37/13/9500/1023311/ef3c00597.pdf by guest on 28 August 2026

https://doi.org/10.1021/acs.energyfuels.3c00597
Energy Fuels 2023, 37, 9500−9513

Table 4. Temperature and Dry Molar Composition in the Exhaust Gas, Predicted by the Numerical Models and Measured in the Experiments for the Cases with ϕ = 0.8 and 0.6

case	data	T_{out} (K)	CH_4 (ppm)	H_2 (ppm)	CO (ppm)	CO_2 (ppm)	O_2 (ppm)
ϕ = 0.8	EXP	1337	<1	36	42	9.62	3.44
	PaSR with C_{mix} = 0.1	1351	0	4	12	9.00	4.57
	PaSR with C_{mix} = 0.5	1335	0	8	37	9.02	4.56
	PaSR with C_{mix} = 1.0	1344	19	20	113	9.02	4.58
	FGM	1329	0	390	916	8.83	4.97
ϕ = 0.6	EXP	1283	<1	<1	<1	7.08	8.11
	PaSR with C_{mix} = 0.1	1372	0	1	6	6.38	8.59
	PaSR with C_{mix} = 0.5	1377	0	4	32	6.44	8.68
	PaSR with C_{mix} = 1.0	1487	7	11	51	6.61	8.90
	FGM	1283	0	9	20	6.05	10.06

become negligible as a result of high contents of oxygen in the burnt gas recirculation.

Conversely, when the O_2 level in the burnt gases is much lower than the H_2O and CO_2 concentrations (i.e., at ϕ > 0.6), FGM accuracy decreases, and this behavior occurs because the reacting mixture ignition close to the exit of the jets is highly influenced by internal dilution effects related to high CO_2 and H_2O concentrations.

A suitable solution to improve FGM accuracy could be to consider a diluted oxidizer stream for the flamelet construction that, however, is beyond the aims of the present work.

Table 4 reports the temperature and major species composition measured for both the experiments and numerical models for the cases with ϕ = 0.8 and 0.6. The emissions are shown on a dry basis. For the case with ϕ = 0.8, there is 1 ppm of CH_4 and few parts per million (ppm) of H_2 and CO in the experimental exhaust gases, indicating complete oxidation of the fuel. The emissions obtained by the PaSR models are in good agreement with the experimental data. It is evident that, by increasing the mixing constant from 0.1 to 1.0, the mixing time becomes longer, leading to lower combustion efficiencies and, thus, higher emissions of unburnt reactants. For the case at ϕ = 0.6, the gas analyzer could not detect any unreacted species, because the large amount of oxygen available in the reactor pushes the conversion toward 100%. In this case, all models are in reasonably good agreement with the experimental values of emission, especially in terms of CH_4 and H_2; in particular, the FGM does not overestimate the species at the exit as in previous cases but presents similar values to those provided by PaSR.

4.5. Combustion Regime Analysis. To comprehensively determine the combustion regime inside the LUCY burner, it is necessary to analyze certain key indicators, such as the temperature field and the Damkhöler number (Da). This number, which is defined as the ratio between mixing and chemical time scales, is commonly used to determine whether the combustion process is limited by mixing and transport or a slow chemistry. In traditional combustion systems, chemistry is generally much faster than mixing, leading to Damkhöler numbers much larger than 1, i.e., $Da \gg 1$, with high temperature gradients. In contrast, advanced combustion systems operating under MILD combustion conditions are typically characterized by intensified mixing and slowed chemistry, resulting in Damkhöler numbers around unity, with uniform temperature distributions.

Figure 11 displays the contours of the Damkhöler number and mixing time scale predicted within the reactor at different equivalence ratios by the PaSR model with C_{mix} = 0.5. It is visible that, in all cases, the Damkhöler number is lower than 1, indicating well-established MILD combustion conditions, consistent with the uniform temperature field observed in Figure 6b and plots b and d of Figure 9. Furthermore, it is worth noting that, as the equivalence ratio diminishes, the mixing time scale and, thus, the Damkhöler number decrease. This happens because turbulence intensifies at φ = 0.8 and 0.6, enhancing mixing. However, the reacting region shifts more upstream as a result of higher concentrations of oxygen available.

5. CONCLUSION

RANS simulations of a lab-scale cyclonic burner, used as a scale-bridging configuration to mimic MILD combustion, fed with methane and air in different proportions were performed with various modeling approaches for turbulence, kinetics, and turbulence−chemistry interactions. Experimental data of the temperature collected in the preheating/ignition zone and in the central zone of the burner midplane as well as measurements of exhaust gas composition were used to test and validate the numerical models. The main outcomes can be summarized as follows: (1) The KEE-58 kinetic mechanism provides the same results as the more detailed GRI-Mech 2.11 but with a lower computational cost; hence, it represents a good choice to describe the methane oxidation kinetics in this case study. (2) The presented models for turbulence show similar temperature profiles, without any remarkable improvement in the accuracy of the prediction when using the more complex RSM. For this reason, RNG $k-\varepsilon$ is chosen to describe turbulence, being more stable and affordable in terms of computational efforts. (3) For the case with ϕ = 1.0, the EDC standard, the EDC with modified constant C_τ = 1.5, and the PaSR model with C_{mix} = 0.5 show similar results, capturing the shape of the experimental profiles of the temperature, resulting in a fairly good agreement. At ϕ = 0.8, the PaSR models still provide sufficiently good results with the experimental data, showing a certain robustness. At ϕ = 0.6, the PaSR models can follow the temperature trends, but the simulations provided a general overestimation of the profiles. (4) At ϕ = 1.0 and 0.8, FGM overpredicts the temperature measurements in the lateral region, showing an early ignition. This can be attributed to the fact that FGM lacks a control variable to consider the dilution as a result of recirculating combustion products. In fact, as the amount of oxygen available in the reactor increases, i.e., at ϕ = 0.6, the FGM accuracy improves, showing a good agreement with the experimental data of the temperature. (5) With regard to the emissions, at ϕ = 1.0, there is a high sensitivity of the combustion efficiency and, thus, of the species emitted to the system temperature. Hence, large discrepancies are registered among the models themselves and with the experimental values. EDC and PaSR models burn at a

Downloaded from pubs.acs.org/energyfuels/article-pdf/37/13/9500/1023331/ef3c00597.pdf by guest on 28 August 2026

https://doi.org/10.1021/acs.energyfuels.3c00597
Energy Fuels 2023, 37, 9500−9513

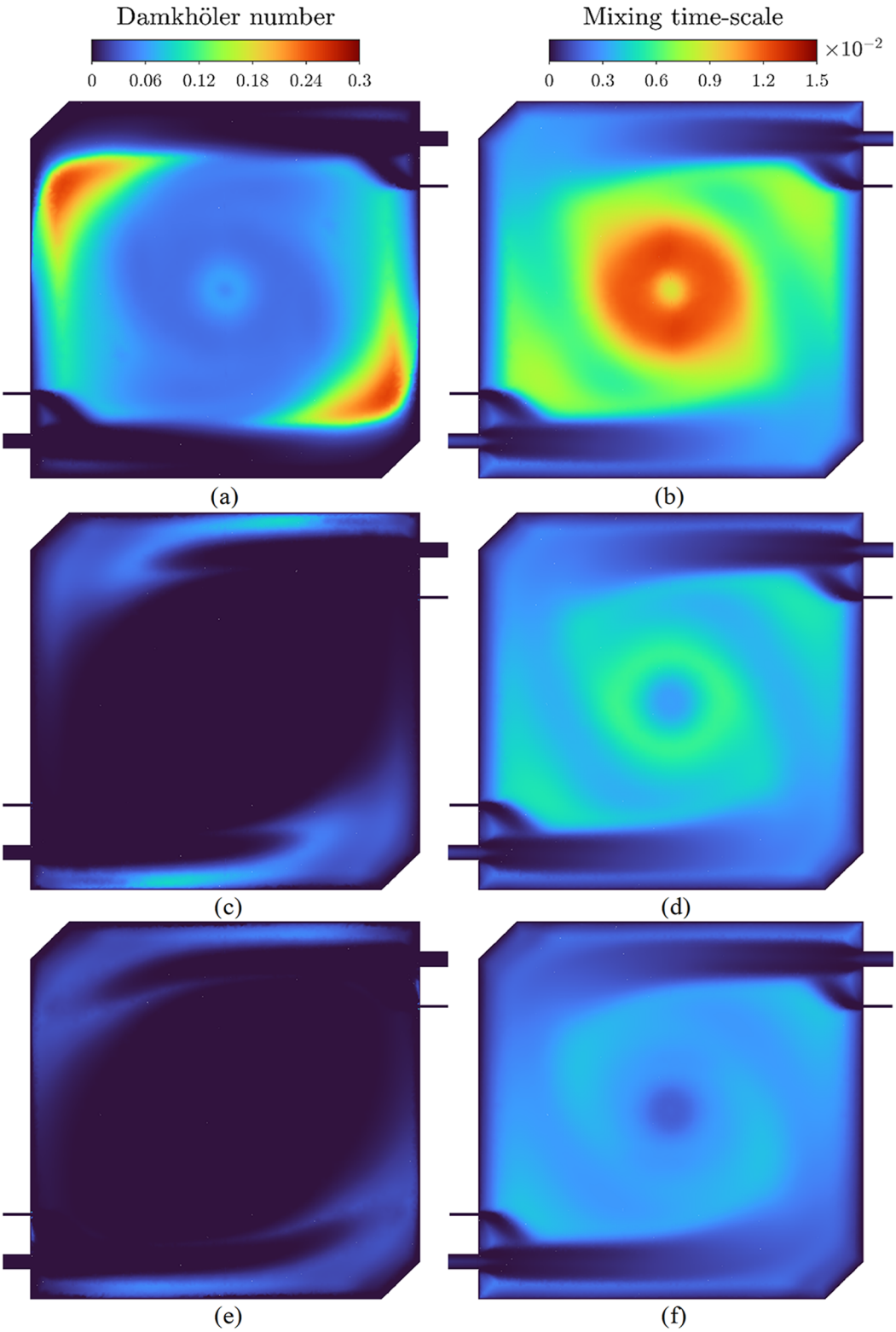


Figure 11. Contours of the Damkhöler number (left) and mixing time scale (right) predicted by PaSR with C_{mix} = 0.5 for the cases at ϕ = 1.0 (plots a and b), ϕ = 0.8 (plots c and d), and ϕ = 0.6 (plots e and f), with KEE-58 as a kinetic scheme and RNG $k-\varepsilon$ as a turbulence model.

slightly higher temperature than the experimental temperature, resulting in lower emission, while FGM burns at a slightly lower temperature, predicting high emissions of unburnt reactants. The experimental values are in the middle. For the cases with ϕ = 0.8 and 0.6, the combustion proceeds to completion thanks to the larger amount of oxygen available. In these case studies, all models predict the experimental emissions reasonably well, with the PaSR model showing the best performances. In conclusion, despite having applied the best available models in the RANS framework, with the PaSR model with $C_{mix} \geq 0.5$ performing the

https://doi.org/10.1021/acs.energyfuels.3c00597
Energy Fuels 2023, 37, 9500−9513

Downloaded from pubs.acs.org/enfuem/article-pdf/37/13/9500/1023311/ef3c00597.pdf by guest on 28 August 2026

best, some discrepancies with the experiments are still present. These limitations can be solved by providing a more accurate treatment of the turbulence−chemistry interactions, for instance, by carrying out hybrid RANS−LES or pure LES analysis, which are, in turn, rather challenging to perform in such a complex configuration.

■ ASSOCIATED CONTENT

Supporting Information

The Supporting Information is available free of charge at https://pubs.acs.org/doi/10.1021/acs.energyfuels.3c00597.

Additional results for section 4.1, performance of detailed kinetic mechanisms, and additional results for sections 4.3 and 4.4, quantitative evaluation of the discrepancies between numerical predictions and experimental data (PDF)

■ AUTHOR INFORMATION

Corresponding Author

Giancarlo Sorrentino − *Institute of Sciences and Technologies for Sustainable Energy and Mobility (STEMS), National Research Council (CNR), 80125 Naples, Italy;* orcid.org/0000-0002-6975-0702; Phone: +39-0812391709; Email: giancarlo.sorrentino@stems.cnr.it

Authors

Lorenzo Giuntini − *Department of Industrial and Civil Engineering, University of Pisa, 56126 Pisa, Italy*

Lorenzo Frascino − *Institute of Sciences and Technologies for Sustainable Energy and Mobility (STEMS), National Research Council (CNR), 80125 Naples, Italy*

Giovanni Battista Ariemma − *Institute of Sciences and Technologies for Sustainable Energy and Mobility (STEMS), National Research Council (CNR), 80125 Naples, Italy; Department of Chemical, Materials and Production Engineering (DICMaPI), University of Naples Federico II, 80125 Naples, Italy*

Chiara Galletti − *Department of Industrial and Civil Engineering, University of Pisa, 56126 Pisa, Italy;* orcid.org/0000-0003-1356-4246

Raffaele Ragucci − *Institute of Sciences and Technologies for Sustainable Energy and Mobility (STEMS), National Research Council (CNR), 80125 Naples, Italy*

Complete contact information is available at: https://pubs.acs.org/10.1021/acs.energyfuels.3c00597

Notes

The authors declare no competing financial interest.

■ REFERENCES

(1) Cavaliere, A.; de Joannon, M. Mild Combustion. *Prog. Energy Combust. Sci.* **2004**, *30* (4), 329−366.

(2) Arghode, V. K.; Gupta, A. K.; Bryden, K. M. High Intensity Colorless Distributed Combustion for Ultra Low Emissions and Enhanced Performance. *Appl. Energy* **2012**, *92*, 822−830.

(3) Sorrentino, G.; Cavaliere, A.; Sabia, P.; Ragucci, R.; de Joannon, M. Diffusion Ignition Processes in MILD Combustion: A Mini-Review. *Front. Mech. Eng.* **2020**, *6*, 10.

(4) Ariemma, G. B.; Bozza, P.; de Joannon, M.; Sabia, P.; Sorrentino, G.; Ragucci, R. Alcohols as Energy Carriers in MILD Combustion. *Energy Fuels* **2021**, *35* (9), 7253−7264.

(5) Sabia, P.; Sorrentino, G.; Ariemma, G. B.; Manna, M. v.; Ragucci, R.; de Joannon, M. MILD Combustion and Biofuels: A Minireview. *Energy Fuels* **2021**, *35*, 19901−19919.

(6) Wünning, J. A.; Wünning, J. G. Flameless Oxidation to Reduce Thermal No-Formation. *Prog. Energy Combust. Sci.* **1997**, *23* (1), 81−94.

(7) Mardani, A.; Tabejamaat, S.; Hassanpour, S. Numerical Study of CO and CO_2 Formation in CH_4/H_2 Blended Flame under MILD Condition. *Combust. Flame* **2013**, *160* (9), 1636−1649.

(8) Szegö, G. G.; Dally, B. B.; Nathan, G. J. Operational Characteristics of a Parallel Jet MILD Combustion Burner System. *Combust. Flame* **2009**, *156* (2), 429−438.

(9) Galletti, C.; Parente, A.; Tognotti, L. Numerical and Experimental Investigation of a Mild Combustion Burner. *Combust. Flame* **2007**, *151* (4), 649−664.

(10) Ferrarotti, M.; Fürst, M.; Cresci, E.; de Paepe, W.; Parente, A. Key Modeling Aspects in the Simulation of a Quasi-Industrial 20 KW Moderate or Intense Low-Oxygen Dilution Combustion Chamber. *Energy Fuels* **2018**, *32* (10), 10228−10241.

(11) Aminian, J.; Galletti, C.; Shahhosseini, S.; Tognotti, L. Key Modeling Issues in Prediction of Minor Species in Diluted-Preheated Combustion Conditions. *Appl. Therm. Eng.* **2011**, *31* (16), 3287−3300.

(12) Parente, A.; Galletti, C.; Tognotti, L. Effect of the Combustion Model and Kinetic Mechanism on the MILD Combustion in an Industrial Burner Fed with Hydrogen Enriched Fuels. *Int. J. Hydrogen Energy* **2008**, *33* (24), 7553−7564.

(13) Evans, M. J.; Medwell, P. R.; Tian, Z. F. Modeling Lifted Jet Flames in a Heated Coflow Using an Optimized Eddy Dissipation Concept Model. *Combust. Sci. Technol.* **2015**, *187* (7), 1093−1109.

(14) Ihme, M.; See, Y. C. LES Flamelet Modeling of a Three-Stream MILD Combustor: Analysis of Flame Sensitivity to Scalar Inflow Conditions. *Proc. Combust. Inst.* **2011**, *33* (1), 1309−1317.

(15) Isaac, B. J.; Parente, A.; Galletti, C.; Thornock, J. N.; Smith, P. J.; Tognotti, L. A Novel Methodology for Chemical Time Scale Evaluation with Detailed Chemical Reaction Kinetics. *Energy Fuels* **2013**, *27* (4), 2255−2265.

(16) Lamouroux, J.; Ihme, M.; Fiorina, B.; Gicquel, O. Tabulated Chemistry Approach for Diluted Combustion Regimes with Internal Recirculation and Heat Losses. *Combust. Flame* **2014**, *161* (8), 2120−2136.

(17) Parente, A.; Malik, M. R.; Contino, F.; Cuoci, A.; Dally, B. B. Extension of the Eddy Dissipation Concept for Turbulence/Chemistry Interactions to MILD Combustion. *Fuel* **2016**, *163*, 98−111.

(18) Aminian, J.; Galletti, C.; Tognotti, L. Extended EDC Local Extinction Model Accounting Finite-Rate Chemistry for MILD Combustion. *Fuel* **2016**, *165*, 123−133.

(19) Lewandowski, M. T.; Parente, A.; Pozorski, J. Generalised Eddy Dissipation Concept for MILD Combustion Regime at Low Local Reynolds and Damköhler Numbers. Part 1: Model Framework Development. *Fuel* **2020**, *278*, No. 117743.

(20) Sorrentino, G.; Ceriello, G.; de Joannon, M.; Sabia, P.; Ragucci, R.; van Oijen, J.; Cavaliere, A.; de Goey, L. P. H. Numerical Investigation of Moderate or Intense Low-Oxygen Dilution Combustion in a Cyclonic Burner Using a Flamelet-Generated Manifold Approach. *Energy Fuels* **2018**, *32* (10), 10242−10255.

(21) Ferrarotti, M.; Li, Z.; Parente, A. On the Role of Mixing Models in the Simulation of MILD Combustion Using Finite-Rate Chemistry Combustion Models. *Proc. Combust. Inst.* **2019**, *37* (4), 4531−4538.

(22) Oldenhof, E.; Tummers, M. J.; van Veen, E. H.; Roekaerts, D. J. E. M. Ignition Kernel Formation and Lift-off Behaviour of Jet-in-Hot-Coflow Flames. *Combust. Flame* **2010**, *157* (6), 1167−1178.

(23) Dally, B. B.; Karpetis, A. N.; Barlow, R. S. Structure of Turbulent Non-Premixed Jet Flames in a Diluted Hot Coflow. *Proc. Combust. Inst.* **2002**, *29* (1), 1147−1154.

(24) Cabra, R.; Chen, J. Y.; Dibble, R. W.; Karpetis, A. N.; Barlow, R. S. Lifted Methane−Air Jet Flames in a Vitiated Coflow. *Combust. Flame* **2005**, *143* (4), 491−506.

Downloaded from pubs.acs.org/enfuem/article-pdf/37/13/9500/1023331/ef3c00597.pdf by guest on 28 August 2026

(25) Oldenhof, E.; Tummers, M. J.; van Veen, E. H.; Roekaerts, D. J. E. M. Role of Entrainment in the Stabilisation of Jet-in-Hot-Coflow Flames. *Combust. Flame* **2011**, *158* (8), 1553−1563.
(26) Sorrentino, G.; Ariemma, G. B.; Manna, M. V.; Cavaliere, A.; Sabia, P.; de Joannon, M.; Ragucci, R. Aerodynamics Issues and Configurations in MILD Reactors. In *Fundamentals of Low Emission Flameless Combustion and Its Applications*; Hosseini, S. E., Ed.; Elsevier: Amsterdam, Netherlands, 2022; Chapter 6, pp 149−180, DOI: 10.1016/B978-0-323-85244-9.00006-X.
(27) Sabia, P.; Sorrentino, G.; Bozza, P.; Ceriello, G.; Ragucci, R.; De Joannon, M. Fuel and Thermal Load Flexibility of a MILD Burner. *Proc. Combust. Inst.* **2019**, *37* (4), 4547−4554.
(28) Ariemma, G. B.; Sorrentino, G.; Ragucci, R.; de Joannon, M.; Sabia, P. Ammonia/Methane Combustion: Stability and NOx Emissions. *Combust. Flame* **2022**, *241*, No. 112071.
(29) Dally, B. B.; Riesmeier, E.; Peters, N. Effect of Fuel Mixture on Moderate and Intense Low Oxygen Dilution Combustion. *Combust. Flame* **2004**, *137* (4), 418−431.
(30) Dally, B. B.; Shim, S. H.; Craig, R. A.; Ashman, P. J.; Szegö, G. G. On the Burning of Sawdust in a MILD Combustion Furnace. *Energy Fuels* **2010**, *24* (6), 3462−3470.
(31) Rebola, A.; Costa, M.; Coelho, P. J. Experimental Evaluation of the Performance of a Flameless Combustor. *Appl. Therm. Eng.* **2013**, *50* (1), 805−815.
(32) Amaduzzi, R.; Ferrarotti, M.; Parente, A. Strategies for Hydrogen-Enriched Methane Flameless Combustion in a Quasi-Industrial Furnace. *Front. Energy Res.* **2021**, *8*, 590300.
(33) Sorrentino, G.; Sabia, P.; Bozza, P.; Ragucci, R.; de Joannon, M. Impact of External Operating Parameters on the Performance of a Cyclonic Burner with High Level of Internal Recirculation under MILD Combustion Conditions. *Energy* **2017**, *137*, 1167−1174.
(34) van Oijen, J. A.; de Goey, L. P. H. Modelling of Premixed Laminar Flames Using Flamelet-Generated Manifolds. *Combust. Sci. Technol.* **2000**, *161*, 113−137.
(35) Magnussen, B. On the Structure of Turbulence and a Generalized Eddy Dissipation Concept for Chemical Reaction in Turbulent Flow. *Proceedings of the 19th Aerospace Sciences Meeting*; St. Louis, MO, Jan 12−15, 1981; DOI: 10.2514/6.1981-42.
(36) Chomiak, J. *Combustion. A Study in Theory, Fact and Application*; Abacus Press: New York, Jan 1, 1990.
(37) Ariemma, G. B.; Sabia, P.; Sorrentino, G.; Bozza, P.; de Joannon, M.; Ragucci, R. Influence of Water Addition on MILD Ammonia Combustion Performances and Emissions. *Proc. Combust. Inst.* **2021**, *38* (4), 5147−5154.
(38) Ariemma, G. B.; Sorrentino, G.; Sabia, P.; Ragucci, R.; de Joannon, M. MILD Combustion of Methanol, Ethanol and 1-Butanol Binary Blends with Ammonia. *Proc. Combust. Inst.* **2023**, *39* (4), 4509−4517.
(39) Launder, B. E.; Reece, G. J.; Rodi, W. Progress in the Development of a Reynolds-Stress Turbulence Closure. *J. Fluid Mech.* **1975**, *68* (3), 537−566.
(40) Bowman, C. T.; Hanson, R. K.; Davidson, D. F.; Gardiner, W. C., Jr.; Lissianski, V.; Smith, G. P.; Golden, D. M.; Frenklach, M.; Goldenberg, M. *GRI-Mech 2.11*; http://combustion.berkeley.edu/gri-mech/new21/version21/text21.html (accessed Feb 15, 2023).
(41) Bilger, R. W.; Stårner, S. H.; Kee, R. J. On Reduced Mechanisms for Methane—air Combustion in Nonpremixed Flames. *Combust. Flame* **1990**, *80* (2), 135−149.
(42) Zhou, C. W.; Li, Y.; Burke, U.; Banyon, C.; Somers, K. P.; Ding, S.; Khan, S.; Hargis, J. W.; Sikes, T.; Mathieu, O.; Petersen, E. L.; AlAbbad, M.; Farooq, A.; Pan, Y.; Zhang, Y.; Huang, Z.; Lopez, J.; Loparo, Z.; Vasu, S. S.; Curran, H. J. An Experimental and Chemical Kinetic Modeling Study of 1,3-Butadiene Combustion: Ignition Delay Time and Laminar Flame Speed Measurements. *Combust. Flame* **2018**, *197*, 423−438.
(43) *Chemical Mechanism: Combustion Research Group at UC San Diego*; https://web.eng.ucsd.edu/mae/groups/combustion/mechanism.html (accessed May 3, 2023).
(44) Fiveland, W. A. Discrete-Ordinates Solutions of the Radiative Transport Equation for Rectangular Enclosures. *J. Heat Transfer* **1984**, *106* (4), 699−706.
(45) ANSYS, Inc. *ANSYS Fluent Theory Guide 15*; ANSYS, Inc.: Canonsburg, PA, 2013.
(46) Smith, T. F.; Shen, Z. F.; Friedman, J. N. Evaluation of Coefficients for the Weighted Sum of Gray Gases Model. *J. Heat Transfer* **1982**, *104* (4), 602−608.
(47) Peters, N. Laminar Diffusion Flamelet Models in Non-Premixed Turbulent Combustion. *Prog. Energy Combust. Sci.* **1984**, *10* (3), 319−339.
(48) Göktolga, M. U.; van Oijen, J. A.; de Goey, L. P. H. 3D DNS of MILD Combustion: A Detailed Analysis of Heat Loss Effects, Preferential Diffusion, and Flame Formation Mechanisms. *Fuel* **2015**, *159*, 784−795.
(49) Maas, U.; Pope, S. B. Simplifying Chemical Kinetics: Intrinsic Low-Dimensional Manifolds in Composition Space. *Combust. Flame* **1992**, *88* (3−4), 239−264.
(50) Aminian, J.; Galletti, C.; Shahhosseini, S.; Tognotti, L. Numerical Investigation of a MILD Combustion Burner: Analysis of Mixing Field, Chemical Kinetics and Turbulence-Chemistry Interaction. *Flow, Turbul. Combust.* **2012**, *88* (4), 597−623.
(51) Amaduzzi, R.; Ceriello, G.; Ferrarotti, M.; Sorrentino, G.; Parente, A. Evaluation of Modeling Approaches for MILD Combustion Systems With Internal Recirculation. *Front. Mech. Eng.* **2020**, *6*, 20.
(52) Ceriello, G.; Sorrentino, G.; Cavaliere, A.; Sabia, P.; de Joannon, M.; Ragucci, R. The Role of Dilution Level and Canonical Configuration in the Modeling of MILD Combustion Systems with Internal Recirculation. *Fuel* **2020**, *264*, No. 116840.
(53) Huang, X.; Tummers, M. J.; van Veen, E. H.; Roekaerts, D. J. E. M. Modelling of MILD Combustion in a Lab-Scale Furnace with an Extended FGM Model Including Turbulence−Radiation Interaction. *Combust. Flame* **2022**, *237*, No. 111634.
(54) Sorrentino, G.; Ceriello, G.; Cavaliere, A.; de Joannon, M.; Ragucci, R. Thermo-Chemical Manifold Reduction for Tabulated Chemistry Modeling. Temperature and Dilution Constraints for Smooth Combustion Reactors. *Proc. Combust. Inst.* **2021**, *38* (4), 5393−5402.
(55) Hu, F.; Li, P.; Guo, J.; Wang, K.; Liu, Z.; Zheng, C. Evaluation, Development, and Validation of a New Reduced Mechanism for Methane Oxy-Fuel Combustion. *Int. J. Greenhouse Gas Control* **2018**, *78*, 327−340.

Downloaded from pubs.acs.org/enfuem/article-pdf/37/13/9500/1023331/ef3c00597.pdf by guest on 28 August 2026